Published in final edited form as:

Virology. 2020 February ; 541: 1–12. doi:10.1016/j.virol.2019.12.002.

The Human Papillomavirus 16 E5 Gene Potentiates MmuPV1-Dependent Pathogenesis

Alexandra D. Torres[a], **Megan E. Spurgeon**[a], **Andrea Bilger**[a], **Simon Blaine-Sauer**[a], **Aayushi Uberoi**[a,*], **Darya Buehler**[b], **Stephanie M. McGregor**[b], **Ella Ward-Shaw**[a], **Paul F. Lambert**[a]

[a]McArdle Laboratory for Cancer Research, Department of Oncology, School of Medicine and Public Health, University of Wisconsin-Madison, 1111 Highland Avenue, Madison, Wisconsin 53705-2275, United States of America

[b]Department of Pathology and Laboratory Medicine, University of Wisconsin School of Medicine and Public Health, Madison, Wisconsin, U.S.A.

Abstract

The papillomavirus E5 gene contributes to transformation and tumorigenesis; however, its exact function in these processes and viral pathogenesis is unclear. While E5 is present in high-risk mucosotropic HPVs that cause anogenital and head and neck cancers, it is absent in cutaneous HPVs and the recently discovered mouse papillomavirus (MmuPV1), which causes papillomas and squamous cell carcinomas of the skin and mucosal epithelia in laboratory mice. We infected *K14E5* transgenic mice, which express the high-risk mucosotropic HPV16 E5 gene in stratified epithelia, with MmuPV1 to investigate the effects of E5 on papillomavirus-induced pathogenesis. Skin lesions in MmuPV1-infected *K14E5* mice had earlier onset, higher incidence, and reduced frequency of spontaneous regression compared to those in non-transgenic mice. *K14E5* mice were also more susceptible to cervicovaginal cancers when infected with MmuPV1 and treated with estrogen compared to non-transgenic mice. Our studies support the hypothesis that E5 contributes to papillomavirus-induced pathogenesis.

Keywords

Human papillomavirus; E5; oncogene; mouse papillomavirus; pathogenesis

INTRODUCTION

Papillomaviruses (PVs) are non-enveloped viruses that contain a double-stranded, circular DNA genome. They infect the stratified squamous epithelium in cutaneous or mucosal tissues and generate benign lesions such as warts that, in some cases, can progress to cancer. Over 180 types of PVs have been identified, delineated by tissue tropism, species specificity,

CORRESPONDING AUTHOR: Paul F. Lambert, plambert@wisc.edu.

*Present address: Aayushi Uberoi, Department of Dermatology, University of Pennsylvania, Philadelphia, Pennsylvania, USA.

and oncogenic potential (Bernard et al., 2010; de Villiers et al., 2004). High-risk, alpha-human papillomaviruses (HPVs), most commonly HPV16, infect mucosal tissue and cause cervical cancer, other anogenital cancers, and a subset of head and neck cancers (zur Hausen, 2002). These high-risk mucosotropic HPVs contain three oncogenes: E5, E6, and E7 (Hawley-Nelson et al., 1989; Leechanachai et al., 1992; Munger et al., 1989; Pim et al., 1992; Straight et al., 1993). The functions of the E6 and E7 oncogenes, which include their inactivation of the cellular tumor suppressors, p53 and pRB, respectively, have been well studied and their contribution to malignancy well-characterized. In contrast, the function of the E5 oncogene is less well understood; though multiple studies have implicated E5 in the viral life cycle (Fehrmann et al., 2003; Genther et al., 2003)(Scott et al., 2019) as well as transformation/tumorigenesis (Bouvard et al., 1994; Crusius et al., 1998; Gu and Matlashewski, 1995; Leechanachai et al., 1992; Leptak et al., 1991; Pim et al., 1992; Straight et al., 1993; Tomakidi et al., 2000; Valle and Banks, 1995).

HPV16 E5 is a hydrophobic, 83 amino acid membrane-associated protein with three transmembrane domains localized to multiple organelles in the cell, such as the Golgi apparatus, endoplasmic reticulum, and nuclear membrane (Bubb et al., 1988; Conrad et al., 1993; Disbrow et al., 2003; Halbert and Galloway, 1988). *In vitro* studies have shown that HPV16 E5 can transform keratinocytes in tissue culture and contribute to increased proliferation of human primary cells (Bouvard et al., 1994; Leechanachai et al., 1992; Leptak et al., 1991; Pim et al., 1992; Straight et al., 1993; Valle and Banks, 1995). E5 expression correlates with increased EGFR activity as well as activation of a signaling pathway (MAPK) downstream of EGFR, upon ligand stimulation, but it is unclear how E5 influences EGFR activity (Conrad et al., 1993; Crusius et al., 1998; Gu and Matlashewski, 1995; Straight et al., 1993; Tomakidi et al., 2000; Zhang et al., 2005).

To study E5 *in vivo*, we previously generated HPV16 E5 (*K14E5*) transgenic mice wherein a codon-optimized version of HPV16 E5 was placed under the transcriptional control of the human keratin 14 (K14) transcriptional promoter, which is active in the basal compartment of stratified squamous epithelia (Genther Williams et al., 2005). Expression of E5 in the cutaneous epithelia of these mice caused overt phenotypes such as wrinkled, scaly skin on the tail and onset of spontaneous skin tumors, as well as histological abnormalities including hyperplasia, hyperkeratosis, increased suprabasal DNA synthesis, and aberrant differentiation. Multiple lines of *K14E5* mice were generated that express different levels of HPV16 E5 and display the E5-associated phenotypes to varying degrees that correlated with the levels of expression of the transgene (Genther Williams et al., 2005). When these mice were crossed to mice that express a dominant negative mutation of *Egfr*, $Egfr^{wa5/+}$, E5-induced hyperplasia was abrogated, providing genetic evidence that E5 acts, at least in part, through EGFR (Genther Williams et al., 2005). When *K14E5* and non-transgenic mice were treated with chemical carcinogens known to induce skin tumors in mice (the tumor initiator DMBA, 7,12-Dimethylbenz(a)anthracene, and the tumor promoter TPA, 12-O-tetradecanoylphorbol-13-acetate), E5 mice developed a higher tumor penetrance, some of which progressed to malignant carcinomas, than non-transgenic mice on the same background, indicating that E5 plays a role in both tumor promotion and tumor progression in skin carcinogenesis (Maufort et al., 2007). When female *K14E5* mice were treated with estrogen, a cofactor for inducing cervical cancers, they displayed more severe neoplastic

disease of the lower female reproductive tract, including cervical/vaginal cancers, than did non-transgenic mice (Maufort et al., 2010). When *K14E5* mice were crossed with *K14E6* or *K14E7* mice that express the HPV16 E6 or E7 oncogenes, respectively, the combined expression of multiple HPV16 oncogenes led to the induction of more severe neoplastic disease of the female reproductive tract (Maufort et al., 2010). These studies provide evidence that HPV16 E5 acts as an oncogene both in the skin and the female reproductive tract.

While the E5 oncogene is present in high-risk alpha-HPVs that infect mucosal tissues, E5 is absent in the genomes of high-risk beta-HPVs that infect cutaneous tissues and that are implicated in skin cancers. E5 is also absent in the recently discovered mouse papillomavirus (MmuPV1) that causes cutaneous warts and squamous cell carcinomas in the skin of laboratory mice. MmuPV1's 7.5kbp circular DNA genome contains the typical set of viral genes, including E6 and E7, with one notable exception; it is missing the E5 gene. Experimental studies with MmuPV1 indicate that it can infect and cause pathogenesis in laboratory mice, thus demonstrating its potential as a useful laboratory infection model for papillomavirus-induced disease (Joh et al., 2011). Though MmuPV1 was originally discovered in cutaneous warts arising in immunocompromised *FoxN1*$^{nu/nu}$ (nude) mice (Ingle et al., 2011), subsequent studies, by our lab and others, reported infections and pathogenesis in immunocompetent mice (Jiang et al., 2017; Spurgeon et al., 2019; Sundberg et al., 2014; Uberoi et al., 2016; Wang et al., 2015). Notably, our lab found that, when a strain of immunocompetent mice (*FVB/NJ*) was irradiated with UVB at the time of MmuPV1-infection, mice developed papillomas on their ears (50% of infected ear sites at 3 months post-infection) whereas this strain of mice was not susceptible to MmuPV1-induced pathogenesis when not UVB-irradiated (Uberoi et al., 2016). The effect of UVB on MmuPV1-induced disease correlated with its ability to induce systemic immunosuppression. A viral dose curve showed a lower penetrance of viral-mediated pathogenesis as the viral dose was decreased, demonstrating that a threshold level of virus is needed to induce MmuPV1-associated disease (Uberoi et al., 2016). Furthermore, MmuPV1 infections generate skin lesions that can progress to squamous cell carcinoma (Uberoi et al., 2016), demonstrating that MmuPV1 may be a useful model to study papillomavirus-induced skin carcinogenesis. More recently, we have determined that MmuPV1 infection of the female reproductive tract of *FVB/N* mice leads to cervicovaginal cancers (Spurgeon et al., 2019). Thus, MmuPV1 is a useful model for studying papillomavirus-induced carcinogenesis at multiple sites in mice.

The observation that E5 is present in some papillomaviruses (high-risk, mucosal, alpha-HPVs), and absent in others (high-risk, cutaneous, beta-HPVs; MmuPV1), led us to question the role of E5 in papillomavirus-associated pathogenesis. We investigated the potential effect of E5 on MmuPV1-induced pathogenesis by infecting *K14E5* transgenic mice with MmuPV1. Upon infection with MmuPV1 at sites of wounding on ears and tails, we observed a markedly earlier onset, higher penetrance and longer persistence of lesions arising at sites of MmuPV1 infection in *K14E5* mice compared to non-transgenic mice on the same genetic background. We also observed that immunocompetent mice, both *K14E5* and non-transgenic mice of the same genetic background, developed skin lesions when infected with a high dose of MmuPV1. Under these conditions, a higher incidence and

earlier onset of skin lesions arose in *K14E5* mice than in non-transgenic mice, similar to what was observed in UVB-treated mice. We also found that *K14E5* mice were more susceptible to MmuPV1-induced carcinogenesis in the female reproductive tract. Together, these results provide compelling evidence that E5 acts as a co-carcinogen in papillomavirus-induced pathogenesis in the context of a natural papillomavirus infection model.

RESULTS

HPV16 E5 expression sensitizes mice to MmuPV1-induced tumorigenesis following exposure to UVB irradiation.

We sought to determine whether HPV16 E5 expression in mice influences MmuPV1-induced cutaneous pathogenesis. Ear and tail sites of *K14E5* transgenic and non-transgenic mice on the same genetic background (*FVB/N*) were scarified to induce wounding in the squamous epithelia of the skin and then topically treated with 10^8 viral genome equivalents (VGE) of MmuPV1 virions (MmuPV1-infected mice) or with the vehicle PBS (mock-infected mice). We infected sites on the ears and tails of the mice because these are the sites known to be susceptible to MmuPV1-induced disease (Handisurya et al., 2013; Sundberg et al., 2014; Uberoi et al., 2016). Mock infections were conducted to determine whether wounding alone was sufficient to induce skin lesions in *K14E5* mice. All mice were then exposed to 300 mJ/cm^2 of UVB whole body irradiation 24 hours post-infection. Because previous studies in our lab had shown that *K14E5* mice can develop spontaneous tumors when allowed to age (Genther Williams et al., 2005; Maufort et al., 2007), we included in our study cohorts of *K14E5* and non-transgenic mice that were not scarified ("Untouched"), to determine whether spontaneous tumors arose in these mice over the time course of our experiments. Mice were observed every other week for lesions, and lesions that arose were measured for their size until the study endpoint. Ear and tail tissues were harvested between 24 and 26 weeks post-infection and examined histopathologically to assess neoplastic disease.

K14E5 mice that were infected with MmuPV1 displayed significantly earlier onset of lesions than did non-transgenic mice infected with MmuPV1 (*K14E5* vs. NTG, $p<0.001$, Log rank test) as well as mock-infected *K14E5* mice (*K14E5* MmuPV1-infected vs. *K14E5* mock-infected, $p<0.05$, Log rank test) (Fig. 1A). No lesions arose in mock-infected non-transgenic mice (n=0/12 sites developed papillomas; Fig. 1A). While the fraction of tumor-free sites in MmuPV1-infected *K14E5* mice was zero (n=24/24 sites developed papillomas) by 16 weeks post-infection, the fraction of tumor-free sites in mock-infected *K14E5* mice (n=4/12 sites developed papillomas) and MmuPV1-infected non-transgenic mice (n=6/36 sites developed papillomas) remained above 0.5 over the course of the study (Fig. 1A). In the absence of MmuPV1 infection, HPV16 E5 expression was sufficient to induce skin lesions in UV-irradiated mice upon wounding, but at a low penetrance (n=4/12 sites). These data demonstrate that HPV16 E5 significantly increases the onset and penetrance of MmuPV1-induced lesions.

Over the time course of the study, average tumor volumes in MmuPV1-infected *K14E5* mice were significantly larger (largest average tumor volume of 5.7 mm^3), and generally increased at a greater growth rate over the course of the study than those arising in

MmuPV1-infected non-transgenic mice (largest average tumor volume of 1.9 mm^3) (*K14E5* vs. NTG, p=0.02, Sen-Adichie test) (Fig. 1B, left). The average maximum tumor volume of individual lesions in *K14E5* mice (average of 6.0 mm^3) was significantly larger than in non-transgenic mice (average of 1.74 mm^3) (*K14E5* vs. NTG, p<0.001, Kruskal-Wallis test) (Fig. 1B, right). Likewise, the growth rates of individual tumors arising in *K14E5* mice were significantly higher than those in non-transgenic mice (*K14E5* vs. NTG, p=0.02, Kruskal-Wallis test) (Fig. 1C). At the study endpoint, 32% of lesions that arose in infected sites in *K14E5* mice were still increasing in volume compared to 17% of lesions in non-transgenic mice, while 5% of lesions in *K14E5* mice fully regressed compared to 83% of lesions in non-transgenic mice (Fig. 1D). There was a significant difference in the extent of regression between *K14E5* mice and non-transgenic mice (*K14E5* vs. NTG, p<0.001, Wilcoxon rank sum) (Fig. 1D, Fig S1). Taken together, these data demonstrate that HPV16 E5 increases the susceptibility of mice to skin lesions induced by MmuPV1 infection and affects tumor regression and persistence in the presence of UVB irradiation.

In the absence of UVB irradiation, high doses of MmuPV1 induce lesions in *K14E5* mice in a dose-dependent manner.

To determine whether MmuPV1 infection was able to induce lesions in *K14E5* transgenic mice and non-transgenic mice in the absence UVB irradiation, ear and tail sites of *K14E5* mice and non-transgenic mice were scarified and infected with 10^{10} VGE of MmuPV1 virions. We chose this higher dose of virus to infect mice in order to increase the likelihood that lesions would arise given that these mice were not exposed to UVB irradiation. Lesions arose in both the ears and tails of *K14E5* and non-transgenic mice, and those arising in *K14E5* mice displayed a significantly earlier onset than in non-transgenic mice (*K14E5* vs. NTG, p<0.001, Logrank test) (Fig. 2A). By week 6, 100% of MmuPV1-infected sites in *K14E5* mice developed a lesion (n=15/15 sites); whereas ~ 55% of infected sites developed a lesion in non-transgenic mice (n=10/18 sites). While there was no significant difference in average tumor volumes of lesions that arose in *K14E5* mice compared to non-transgenic mice (*K14E5* vs. NTG, p=0.2, Sen-Adichie test) (Fig. 2B, left), there were significant differences in the maximum tumor volumes of individual lesions (*K14E5* vs. NTG, p<0.005, Kruskal-Wallis test) (Fig. 2B, right) as well as the tumor growth rates (*K14E5* vs. NTG, p<0.001, Kruskal-Wallis test) (Fig. 2C) in *K14E5* mice compared to non-transgenic mice. There was no difference in the extent of regression of lesions between *K14E5* mice and non-transgenic mice, with a little less than half of lesions still increasing in volume at the study endpoint (44% of *K14E5* mice, 46% of NTG mice) and a little over half of lesions partially regressing (56% of *K14E5* mice, 54% of NTG mice) (*K14E5* vs. NTG, p>0.05, Wilcoxon rank sum) (Fig. 2D).

We next wanted to determine whether decreasing the viral dose of MmuPV1 virions during infection would identify a threshold level of virus that is needed to induce lesions in *K14E5* or non-transgenic mice in the absence of UVB. We therefore conducted infections in which ear and tail sites of *K14E5* or non-transgenic mice that were exposed to 10^9 or 10^8 VGE of MmuPV1. As expected, we saw a trend towards later onset of lesions arising in both *K14E5* and non-transgenic mice as the viral dose was decreased (Fig. S2). In addition, we observed that, within each infection dose, tumor onset in *K14E5* mice was significantly earlier than in

non-transgenic mice (*K14E5* vs. NTG, 10^9 VGE p<0.001, 10^8 VGE p<0.004, Logrank test; Fig. S2). While complete tumor penetrance was achieved in *K14E5* mice infected with each dose, this was not the case in non-transgenic mice. While there were significant differences in the maximum tumor volumes and tumor growth rates between *K14E5* and non-transgenic mice infected with 10^{10} VGE (Fig. 2), there were no significant differences in either of these parameters in the mice infected with 10^9 or 10^8 VGE (data not shown). Interestingly, while there was no difference in the extent of regression between *K14E5* and non-transgenic mice infected with either 10^{10} or 10^9 VGE of MmuPV1, lesions that arose in *K14E5* mice infected with 10^8 VGE underwent less regression (29% of lesions were increasing and 71% of lesions had partially regressed) than in non-transgenic mice (42% of lesions had partially regressed and 58% of lesions had fully regressed), indicating a trend towards greater regression in non-transgenic mice as the viral dose is decreased (*K14E5* vs. NTG, 10^8 VGE p<0.001, Wilcoxon rank sum; data not shown). Together, these data indicate that HPV16 E5 also contributes to MmuPV1-induced cutaneous pathogenesis in the absence of UVB.

E5 expression alone is sufficient to induce skin lesions both in UV-irradiated and non UV-irradiated mice upon wounding.

To determine whether wounding alone was sufficient to induce skin lesions in *K14E5* and non-transgenic mice, either in the presence or absence of UVB irradiation, ear and tail sites of *K14E5* and non-transgenic mice were scarified in the same manner as for MmuPV1 infections, but instead of applying a solution containing virions, only a PBS solution was applied to the wounded site. Subsets of these mice were exposed to 300mJ/cm^2 of whole body UVB irradiation 24 hours post scarification. Additionally, because previous studies in our lab have shown that *K14E5* mice develop spontaneous tumors when allowed to age (Genther Williams et al., 2005; Maufort et al., 2007), we also held cohorts of both *K14E5* and non-transgenic mice over the course of our study that were not scarified ("Untouched") on their ears or tails to determine whether spontaneous tumors arose in those mice during the time course.

Both UVB-irradiated and non UVB-irradiated *K14E5* mock-infected mice developed skin lesions at the sites of wounding; whereas, neither UVB-irradiated nor non UVB-irradiated non-transgenic mice developed lesions (Table 1). We compared the properties of lesions that arose in the mock-infected UVB-irradiated *K14E5* mice to those that arose in virus-infected (10^8 VGE) UVB-irradiated mice as well as lesions that arose in mock-infected unirradiated mice to those that arose in virus-infected (10^{10} VGE) unirradiated mice. In both UVB-irradiated and unirradiated mice, there were significant differences in tumor onset, with lesions at virus-infected sites appearing earlier than lesions at mock-infected sites (*K14E5* mock-infected vs. *K14E5* virus-infected, with UV p<0.05, No UV p<0.001, Logrank test) (Fig. 1, Fig. 2). There also was a significant difference in tumor volume over time when mice were treated with UV (*K14E5* mock-infected vs. *K14E5* virus-infected, p<0.01, Sen-Adichie test), but this was not observed in the non UVB-treated groups (p>0.05, Sen-Adichie test) (data not shown). Regardless of UVB treatment, there were significant differences in maximum volume of tumors (*K14E5* mock-infected vs. *K14E5* virus-infected, UV p=0.02, No UV p=0.003, Kruskal-Wallis test) (data not shown) and growth rates (*K14E5* mock-infected vs. *K14E5* virus-infected, UV p=0.01, No UV p=0.001, Kruskal-

Wallis test) (data not shown). *K14E5* mice that were infected with MmuPV1 had a significantly greater proportion of lesions that were still increasing in size or had partially regressed compared to *K14E5* mice that were mock-infected, which had more lesions that fully regressed (*K14E5* mock-infected vs. *K14E5* virus-infected, UV $p<0.05$, No UV $p=0.01$, Wilcoxon rank sum) (data not shown). Over the course of our study, neither untouched *K14E5* mice nor untouched non-transgenic mice developed lesions (Fig. 2).

In sum, when MmuPV1 virus is present at the site of wounding in *K14E5* mice, lesions appear earlier, grow faster, and are generally larger in size than in non-transgenic mice. However, E5 alone is sufficient to induce skin tumors in mice upon wounding, albeit with reduced efficiency.

Lesions that arise in E5-expressing mice display more aggressive neoplastic progression.

At the study endpoint, sites of infection/mock infection were harvested and processed for histopathological analysis. Tissue sections were stained with hematoxylin and eosin (H&E) and a subset of the sites of infection underwent detailed histopathological analysis to determine the worst stage of neoplastic disease in each tissue (Table 1). For mock-infected sites, at which there was no detectable overt disease at the endpoint, a minimum of 3 randomly selected samples were histologically analyzed. For infected sites, at which a range of overt disease was obvious at the endpoint depending on the group, a minimum of 5 randomly selected sites were histologically analyzed. Sites of MmuPV1 infection in *K14E5* mice displayed a range of progressive disease that extended from a normal epithelium to keratosis, to dysplasia, to cancer (squamous cell carcinoma; SCC). Dysplasia was subcategorized into low, moderate, and high grades of dysplasia and SCC was delineated by the degree of invasiveness (minimally invasive vs. invasive). At the endpoint of the study, none of the sites of infection in UVB-irradiated, MmuPV1-infected (10^8 VGE) non-transgenic mice displayed any form of dysplasia or SCC (0/5). However, 5 out of 8 infected sites in UVB-irradiated MmuPV1-infected *K14E5* mice progressed to carcinomas and 2 out of 8 were dysplastic (*K14E5* virus-infected vs. NTG virus-infected, $p<0.01$, two-sided Wilcoxon rank sum test) (Table 1). Neoplastic disease was also worse in *K14E5* mice versus non-transgenic mice in the absence of UVB irradiation. In non UVB-irradiated MmuPV1-infected (10^{10} VGE) *K14E5* mice, 3 out of 6 sites analyzed were carcinomas and the other 3 sites were dysplastic; whereas in non-transgenic mice, 2 out of 6 sites were carcinomas and 3 out of 6 were dysplastic (*K14E5* virus-infected vs. NTG virus-infected, $p=0.4$, two-sided Wilcoxon rank sum test) (Table 1).

No mock-infected sites, either in *K14E5* or non-transgenic mice, progressed to cancer (Table 1). The only indication of progressive disease seen in mock-infected samples was in one site (n=1/3) in the UVB-treated, mock-infected K14E5 mice that showed keratosis and 3 out of 8 sites in non UVB-irradiated, mock-infected *K14E5* mice which displayed low grade dysplasia (Table 1). No sign of neoplastic disease was seen in untouched *K14E5* or non-transgenic mice (data not shown). These histopathological observations indicate that E5 increases the severity of neoplastic disease in MmuPV1-infected mice.

MmuPV1-infected lesions arising in *K14E5* mice display similar levels of productive viral infection to that seen in lesions arising in FVB mice.

To determine whether MmuPV1-infected sites display a productive viral infection, we looked for the presence of the MmuPV1 major viral capsid protein, L1, in the tissues harvested at the endpoint by indirect immunofluorescence. L1-positive cells were not observed in any mock-infected sites in either *K14E5* or non-transgenic mice in both the UVB-treated (Fig. 3A), and non-UVB-treated (Fig. 4A) cohorts. No L1-positive cells were observed in the infected sites of MmuPV1-infected non-transgenic mice irradiated with UVB (infected with 10^8 VGE), consistent with these sites not showing any dysplasia or cancer at the endpoint; however, L1-positive cells were observed in 2 out of 8 MmuPV1-infected sites in *K14E5* mice irradiated with UVB (infected with 10^8 VGE) that retained dysplastic histopathology at the endpoint (Fig. 3B). In the cohorts infected with 10^{10} VGE and not UVB irradiated, L1-positive cells were observed in the 3 out of 6 MmuPV1-infected sites in non-transgenic mice that displayed dysplasia at the endpoint and 6 out of 6 MmuPV1-infected sites in *K14E5* mice that displayed dysplasia (Fig. 4B). Differences in the presence of L1 between MmuPV1-infected sites of non-transgenic and K14E5 mice were not statistically significant (*K14E5* virus-infected vs. NTG virus-infected, UVB-irradiated $p=0.4$, non UVB-irradiated $p=0.09$, respectively). We conclude that HPV16 E5 does not have a demonstrable effect on the productive phase of the MmuPV1 life cycle.

HPV16 E5 gene expression exacerbates disease in estrogen-treated MmuPV1-infected female reproductive tracts of *K14E5* transgenic mice.

We recently reported that *FVB/N* wild-type mice are susceptible to MmuPV1-induced neoplastic progression in the mucosal epithelia of the female reproductive tract (Spurgeon et al., 2019). We found that UV radiation and the female hormone estrogen, two cofactors previously identified as being involved in papillomavirus-mediated disease in other murine models (Brake and Lambert, 2005; Chung et al., 2008; Riley et al., 2003; Uberoi et al., 2016), contribute to MmuPV1 infection and malignant progression in this cervicovaginal infection model. At 4 months post-infection, estrogen treatment significantly increased the severity of disease in *FVB* mice infected with MmuPV1, and mice developed SCC in the lower reproductive tract when treated with both estrogen and UVB irradiation. We therefore sought to determine if HPV16 E5 gene expression in the mucosal epithelia of *K14E5* mice has a similar positive effect as was observed in cutaneous epithelia on MmuPV1 pathogenesis and neoplastic progression, either alone or in combination with UV and/or estrogen, in the female reproductive tract.

Four different groups of *FVB* and *K14E5* mice were included in this study: (i) MmuPV1 only (10^8 VGE/mouse), (ii) MmuPV1-infected mice irradiated with 1000 mJ/cm^2 UVB (MmuPV1+UVB), (iii) MmuPV1-infected mice treated with exogenous estrogen (E2) (0.05 mg 17β-estradiol over 60 days; MmuPV1+E2), and (iv) MmuPV1-infected mice that were UVB-irradiated and treated with exogenous estrogen (Fig. 5A). Mock-infected controls were treated identically, but were not infected with MmuPV1. At 4 months post-infection, tissue was harvested and evaluated histopathologically to score for worst disease. Disease was determined for the vagina and cervix separately for *FVB* (Table S1) and *K14E5* (Table S2) mice. Consistent with our previous findings (Spurgeon et al., 2019), sites of disease

correlated with exposure to the virus inoculum, and we therefore analyzed disease severity by combining the cervical and vaginal scores and present the worst stage of disease in the whole of the cervicovaginal tissue for each mouse (Fig. 5B).

Infection of the cervicovaginal tract with MmuPV1 caused neoplastic disease in both *FVB* and *K14E5* mice. We first compared the overall cervicovaginal disease severity between infected groups of mice and their mock-infected counterparts. In the absence of cofactor treatment, the severity of disease in *FVB* and *K14E5* mice infected with MmuPV1 was not significantly higher than mock-infected controls (Mock vs. MmuPV1: *FVB*, p=0.59; *K14E5*, p=0.53). The same was true for both *FVB* and *K14E5* MmuPV1-infected mice irradiated with UVB (Mock+UVB vs. MmuPV1+UVB*: FVB*, p=1.0; *K14E5*, p=0.36). Treatment with estrogen, or estrogen in combination with UVB, significantly increased disease in both *FVB* (Table S1) and *K14E5* (Table S2) mice compared to mock-infected controls (Mock+E2 vs MmuPV1+E2: *FVB*, p=0.05; *K14E5*, p=0.05 and Mock+UVB+E2 vs. MmuPV1+UVB+E2: *FVB*, p=0.03; *K14E5,* p=0.05). In *K14E5* MmuPV1-infected mice, estrogen alone and estrogen plus UVB also significantly increased disease severity compared to disease in mice only infected with MmuPV1 (Fig. 5B). Therefore, the mucosal cervicovaginal epithelia in *K14E5* transgenic mice supported MmuPV1 infection and subsequent neoplastic disease, and treatment with estrogen, alone or in combination with UVB, exacerbated disease in both *FVB* and *K14E5* mice compared to mock-infected controls.

We next compared disease severity between cohorts of MmuPV1-infected *FVB* and *K14E5* mice to determine whether HPV16 E5 expression affected overall disease severity (Fig. 5B). We observed a significant effect of HPV16 E5 expression in MmuPV1-infected mice treated with exogenous estrogen (*FVB* vs. *K14E5* MmuPV1+E2, p=0.05). In MmuPV1+E2 *FVB* mice, one of three mice developed moderate dysplasia, and the remaining two developed high-grade dysplasia. In contrast, all three MmuPV1+E2 *K14E5* mice developed SCC. In the other treatment groups (MmuPV1, MmuPV1+UVB, MmuPV1+UVB+E2), we did not see significant differences (Fig. 5B). HPV16 E5 expression in MmuPV1 only-infected mice did not significantly increase disease severity (*FVB* vs. *K14E5* MmuPV1 only, p=1.0). Likewise, HPV16 E5 expression did not significantly increase disease severity in MmuPV1-infected mice treated with UVB (*FVB* vs. *K14E5* MmuPV1+UVB, p=0.58). All MmuPV1+UVB+E2 *K14E5* mice developed SCC compared to 75% (n=3/4) of the MmuPV1+UVB+E2 *FVB* mice (*FVB* vs. *K14E5* MmuPV1+UVB+E2, p=0.59). We conclude that, in the presence of estrogen alone, HPV16 E5 increased neoplastic severity of disease caused by MmuPV1.

Immunofluorescence staining for the MmuPV1 capsid L1 protein confirmed that *K14E5* supported productive viral infections in the mucosal epithelia of the female reproductive tract (Fig. 5C). We did not observe significant differences in the level or intensity of L1 staining between *FVB* and *K14E5* mice, consistent with our findings in cutaneous sites. While we only observed a statistically significant increase in overall disease severity in MmuPV1+E2 *K14E5* mice versus *FVB* mice (Fig. 5B), the histopathology associated with high-grade dysplasias and SCCs that developed in *K14E5* suggests HPV16 E5 protein expression contributes to more advanced tumor burden and more aggressive disease compared to disease in *FVB* mice (Fig. 5D). Future studies are necessary to determine the

mechanisms underlying this observation, and why the functions of HPV16 E5 appear to synergize with co-carcinogens differently in MmuPV1-induced cutaneous and mucosal disease.

DISCUSSION

In this study, we demonstrate that expression of HPV16 E5 increases the susceptibility of mice infected with MmuPV1 to progressive neoplastic disease in both the skin and female reproductive tract. This is an important finding that builds upon previous *in vivo* work done in our lab on HPV16 E5 that support its role as an oncogene, this time in the context of a papillomavirus that does not normally express E5, MmuPV1. Our work supports the hypothesis that E5 contributes to papillomavirus-induced pathogenesis.

How does E5 potentiate MmuPV1-induced pathogenesis?

There are a number of mutually non-exclusive hypotheses for why E5 can potentiate MmuPV1-induced disease. One hypothesis is that E5 provides a more amenable environment within epithelial cells for initial infection. For papillomaviruses to establish their genomes in epithelial cells, the infected cell must pass through mitosis (Pyeon et al., 2009). We have previously shown that E5 drives proliferation of epithelial cells *in vivo* in *K14E5* mice through its activation of EGFR (Genther Williams et al., 2005). Consistent with this hypothesis, *K14E5* mice displayed increased incidence of cutaneous papillomas (Fig. 1; Fig. 2; Fig S2). A related, second hypothesis is that increased hyperplasia caused by E5 could help MmuPV1-infected cells to expand in numbers. Consistent with this hypothesis, MmuPV1-induced cutaneous lesions grew faster and achieved larger tumor volumes in *K14E5* transgenic mice (Fig 1; Fig 2). A third hypothesis is that E5 potentiates the productive phase of the viral life cycle (Genther et al., 2003). Our results do not strongly support this hypothesis as the level of L1 staining in cutaneous and mucosal lesions arising in FVB and K14E5 mice were not significantly different (Zhang et al., 2003). Consistent with this hypothesis, we observed reduced frequency of regression of MmuPV1-induced cutaneous warts in *K14E5* transgenic mice (Fig. 1D; Fig. 2D; Fig S1). A fifth hypothesis is that E5 overcomes the proposed restrictive properties of *Ever* genes on papillomavirus infection, as E5 has been shown to interact with *EVER* gene products (Lazarczyk et al., 2008). *EVER* genes are mutated in patients suffering from epidermodysplasia verruciformis. These patients display increased susceptibility to infection by certain beta-HPVs, and these beta-HPV-induced skin lesions can progress to cancer at sun-exposed sites. It has been argued that beta-HPVs are restricted in their ability to infect *EVER*-wild type humans because they lack an E5 gene that can interfere with *EVER* functions. Additional studies will be necessary to test further these different hypotheses.

Why did lesions arise at mock-infected cutaneous sites on *K14E5* transgenic mice?

We observed that overt lesions arose at a fraction of mock-infected cutaneous sites on *K14E5* transgenic mice, but did not develop on untouched *K14E5* mice nor mock-infected non-transgenic mice. Likewise, we did not observe significant pathology in the reproductive tracts of mock-infected *K14E5* mice. We conclude that wounding alone can lead to the development of skin lesions in *K14E5* mice. These lesions, however, were short-lived, with

most regressing by the endpoint of the study. In mock-infected *K14E5* mice where a lesion had arisen, 3 out of 11 sites showed pathology at the endpoint and those sites were scored as being hyperplastic but benign. Nevertheless, it is interesting that lesions arose at all. We have previously observed that wounding can lead to increased susceptibility of warts arising in HPV16 transgenic mice expressing E6 and E7 (Lambert et al., 1993). It remains unclear how the wounding process synergizes with papillomavirus oncogenes to induce lesions on the skin. Lesions in *K14E5* mice were short-lived, which may indicate that the wound healing process combined with the ability of E5 to induce hyperplasia led to a greater than normal expansion of epithelial cells that returned to normal homeostasis over time in most cases.

Ability of MmuPV1 to cause warts in the absence of UVB.

In prior studies, we and others have observed that immunocompetent mice, including the *FVB* strain, are reduced in their susceptibility to MmuPV1-induced pathogenesis compared to immunodeficient mice, and we found that UVB increases susceptibility of *FVB* and *C57BL/6* mice to MmuPV1-induced pathogenesis at least in part by inducing systemic immunosuppression (Uberoi et al., 2016). It was therefore surprising that non-transgenic *FVB* mice developed warts when infected with high titers of MmuPV1 in the absence of UVB. Other recent studies in our lab have recapitulated this finding (Wang et al., *PLoS Pathogens*, accepted).

We have discounted the possibility that the virus has evolved through genetic changes to become more capable of infecting immunocompetent mice. We sequenced multiple independent stocks of MmuPV1 that all give rise to warts in non UVB-treated FVB mice; all were identical in their sequence to the original clone (Denis Lee, unpublished data). We believe the difference may reflect the fact that the stocks of virus we currently generate are more infectious. This is based upon quantitative E1Ê4 viral mRNA-specific RT-PCR analyses of virus-infected mouse keratinocytes *in vitro* (Wei Wang, unpublished results). Why this is the case remains unclear. Perhaps there are epigenetic differences that contribute to increased infectivity, or that the current preparations of virus do not contain some contaminating substance(s) that inhibits the efficiency of infection. Regardless, we now have the ability to efficiently induce MmuPV1-associated pathogenesis in an immunocompetent strain of mice without inducing immunosuppression. This is important because it now allows us to study the role of an intact immune system on viral pathogenesis.

HPV E5 and cervicovaginal disease in MmuPV1-infected mice

We found that the female reproductive tracts of *K14E5* transgenic mice expressing the HPV16 E5 gene support MmuPV1 infection and subsequent neoplastic progression (Fig. 5). Interestingly, disease severity was similar to *FVB* mice in those animals infected with MmuPV1 alone, MmuPV1+UVB, and MmuPV1+UV+E2. The only treatment regimen in which the HPV16 E5 gene had a significant effect was in MmuPV1-infected mice treated with estrogen. Previous work in our laboratory found that the HPV16 E5 gene alone, without MmuPV1 infection, induces cancer in combination with exogenous estrogen (Maufort et al., 2010). In this study, mock-infected, estrogen-treated *K14E5* mice did not develop significant disease. This discrepancy is likely due to the fact that we have used a transgenic line that expresses lower levels of E5 (Line 33) in this study, while a higher expressing E5 line (Line

32) was used in the previous study. Also, we limited our observation to a 4-month time period in these MmuPV1 infection, compared to 9 months in the prior study. Nonetheless, the results presented here are consistent with our previous work that establishes a role for estrogen in papillomavirus-mediated disease and a synergy with papillomavirus oncogenes.

We saw no effect of HPV16 E5 expression on disease severity in *K14E5* mice infected with MmuPV1 only and MmuPV1+UVB in the female reproductive tract mucosal epithelia, which differs from results in the cutaneous epithelia, in which E5 expression significantly increased skin tumorigenesis in both unirradiated and UVB-irradiated *K14E5* mice. These findings may reflect a different requirement for E5 expression during papillomavirus infection and pathogenesis in cutaneous versus mucosal anatomical sites. Although the context differed (cutaneous vs. mucosal, cofactor treatment), we observed that the HPV16 E5 gene increased disease aggressiveness in both the skin (Table 1) and female reproductive tract in mice treated with estrogen (Fig. 5D). This observation may suggest that the HPV16 E5 gene is indeed contributing some function(s) that the MmuPV1 viral proteins lack. It will be interesting to determine whether the effects of E5 on MmuPV1-associated cutaneous and mucosal disease are EGFR-dependent, as we have seen previously in HPV16 E5 transgenic mice (Genther Williams et al., 2005). Such studies have the potential to further our understanding of the HPV E5 gene function in papillomavirus-mediated cutaneous and mucosal infections and neoplastic progression.

MATERIALS AND METHODS

Animals

The generation and characterization of *K14E5* transgenic mice has been previously described (Genther Williams et al., 2005). Of the multiple lines generated, line 33 was used in these studies. Line 33 displays relatively low levels of E5 in the skin epithelium, and minimal gross phenotypes compared to other lines generated. *K14E5* mice were maintained on the *FVB/N* inbred genetic background in the homozygous state. Genotyping was carried out as previously described (Genther Williams et al., 2005). Non-transgenic *FVB/N* (Taconic) mice were purchased and bred to provide non-transgenic, syngeneic mice as controls for our studies.

All mice were housed in micro-isolator cages. Animals were handled by designated personnel and personal protection gear was used. Mice were fed with the 2019 Teklad rodent diet (Envigo), and maintained on a 12-hour light/12-hour dark cycle. Mice were housed at the Medical Sciences Center Vivarium or the Clinical Sciences Center Vivarium at the University of Wisconsin-Madison School of Medicine and Public Health in strict accordance with guidelines approved by the Association for Assessment of Laboratory Animal Care. All protocols for animal work were approved by the University of Wisconsin-Madison School of Medicine and Public Health Institutional Animal Care and Use Committee (Protocol number M005871).

Cutaneous and cervicovaginal MmuPV1 infections

In vivo infections were performed using purified MmuPV1 virus stocks that were generated by isolating MmuPV1 virions from papillomas in nude mice as described previously (Uberoi et al., 2016). Virus stocks used for cutaneous and reproductive tract infections were isolated from independent warts. The concentration of virus in stocks was quantified by determining the amount of encapsidated viral DNA to give viral genome equivalents (VGE). For any particular experiment, the same stock of virus was used for all cohorts in that experiment. Within any experiment, controls were included for direct comparison. To conduct an infection of cutaneous sites, mice were anesthetized and the skin on the inner ear or tail was scarified using a 27-gauge syringe needle to scrape the skin to disrupt the epithelial tissue. Following scarification, the virus or mock solution (PBS) was delivered to wounded sites by pipette delivery. A detailed description of this infection model has been previously published (Uberoi et al., 2016).

Infections of the female reproductive tract have been described previously (Spurgeon et al., 2019). Briefly, mice were injected subcutaneously with 3 mg medroxyprogesterone acetate (Amphastar Pharmaceuticals, Rancho Cucamongo, CA) 4 days prior to MmuPV1 infection to induce diestrus. On the day of the infection, mice were pre-treated vaginally with 50 μL Conceptrol (Options, #247149) containing 4% nonoxynol-9 to induce chemical injury to the cervicovaginal epithelium. At 4 hours post-treatment with contraceptrol, 10^8 VGE MmuPV1 virions suspended in 25 μL 4% carboxyl methylcellulose (Sigma, #C4888) were delivered intravaginally. All treatments were performed while mice were anesthetized with 5% isoflurane.

UV treatment

Mice that were irradiated were exposed to a single dose of UVB radiation using a Research Irradiation Unit (Daavlin, Bryan, OH). With this system, dose units are entered in milli-Joules per centimeter square for UVB (mJ/cm^2). For cutaneous studies, mice were exposed to 300 mJ/cm^2 of UVB radiation 24 hours post-infection with MmuPV1 or mock solution. For cervicovaginal studies, mice were irradiated 24 hours post-infection with 1000 mJ/cm^2 of UVB.

Estrogen treatment

Treatment with exogenous estrogen was performed as described previously (Arbeit et al., 1996; Elson et al., 2000). Briefly, female mice were anesthetized with 5% isoflurane, and a continuous-release estrogen (E2) tablet (17β-estradiol; 0.05 mg/60 days; Innovative Research of America, Sarasota, FL) was inserted subcutaneously in the shoulder fat pads of the dorsal skin. For those mice receiving estrogen, treatment began 5 days following MmuPV1 infection. A new tablet was inserted every 2 months as needed.

Monitoring of cutaneous tumor presence and tumor volume

Mice were examined every two weeks for the development of lesions at infected cutaneous sites over the course of 6 months. Tumor incidence was noted and tumor volume was measured either by a micrometer or by calipers. For each tumor, four separate measurements were taken: 1) height of tumor on the ear/tail, 2) height of ear/tail in nearby non-infected

region, 3) length of tumor, 4) width of tumor. For each lesion, the largest area of the tumor was measured. To calculate tumor volume, we generated a geometric mean diameter (GMD), as described previously, by subtracting the height of the ear/tail in the non-infected nearby region (2), from the height of the ear/tail at the site of the tumor (1), and multiplying this by the length and width of the tumor. We then took the cubed root of that measurement [$\sqrt[3]{(2–1)\ (3)\ (4)}$] (Cladel et al., 2008). Data are represented as individual tumor measurements or as the mean +/− the standard errors of the mean of the GMDs for each test group. The tumor growth rate was determined by taking the tumor volume at the time of onset and at the next measurement time point and determining the growth rate of the tumor between these two time points. Animals with lesions that had become ulcerated were euthanized for humane reasons. Otherwise, animals were euthanized at the 6-month endpoint.

Tissue Procurement, Processing, and Histopathological Analysis

Tissues were harvested, fixed in 4% paraformaldehyde, processed through a series of ethanol and xylene, and paraffin-embedded. Serial sections (5 μm) were cut and every 10th section was stained with H&E and evaluated by histopathological analysis and scored for worst disease by trained pathologists in the Department of Pathology and Laboratory Medicine (University of Wisconsin-Madison School of Medicine and Public Health), who were blinded to sample genotypes and treatments. Grading of cutaneous disease was performed by Dr. Darya Buehler. Reproductive tract disease was evaluated by Dr. Stephanie McGregor. A detailed overview of the histological scoring criteria in the MmuPV1-infected reproductive tract has been previously described (Spurgeon et al., 2019).

MmuPV1 L1- cytokeratin dual immunofluorescence and immunohistochemistry

Serial sections were subjected to immunofluorescence staining for the MmuPV1 major viral capsid protein, L1 and cytokeratin 14 (CK14). A detailed protocol is available at: dx.doi.org/10.17504/protocols.io.i8cchsw. Briefly, sections were deparaffinized in xylene, then rehydrated with graded ethanol. Antigen retrieval was performed for 20 minutes in buffer (Tris-EDTA buffer pH 6.0; Abcam ab93684). Samples were blocked for 1 hour at ambient temperature in blocking buffer (Perkin Elmer). The primary antibodies used are as follows: anti-MmuPV1 L1 for 12 hours at 4°C (1:1000; gift from Dr. Chris Buck, NCI), anti-Keratin 14 for 1 hour at room temperature (1:1000; Biolegend/Covance). We performed Tyramide Signal Amplification (TSA) to detect MmuPV1 L1. For this, L1 signals were detected first with HRP against rabbit antibody. Then a biotin-tyramide solution (stock at 1mg/ml; 1:100 in reaction buffer: 0.001% H_2O_2 in 0.1M Imidazole) was placed on the tissue for 10 min at room temp. L1-specific TSA signals were detected with streptavidin conjugated to Alexa-fluor 488 or Alexa-fluor 647. K14 signals were detected with a secondary rabbit antibody conjugated to Alexa-fluor 594 or Alexa-fluor 488. Nuclei were counterstained with DAPI for 10 min, and the tissue cover slipped with mounting media. All images were captured using a Zeiss AxioImager M2 microscope using AxioVision software (Jena, Germany).

Statistical analysis

The Logrank test was used to determine the significance of differences in cutaneous tumor onset. The Sen-Adichie test was used to determine the significance of differences in tumor

growth over time. The Kruskal-Wallis test was used to determine the significance of differences in tumor growth rate and maximum tumor volume. The Wilcoxon rank sum test was used to determine the significance of differences in tumor regression and disease severity. To determine the significance of differences of MmuPV1 L1-positive cells between each group of mice, the Fisher's exact test was used. Statistical analysis was carried out using the Mstat program (available from: http://www.mcardle.wisc.edu/mstat/).

Supplementary Material

Refer to Web version on PubMed Central for supplementary material.

ACKNOWLEDGEMENTS

We thank Dr. Chris Buck (National Cancer Institute, Bethesda, MD) for providing us with antibody against L1. We thank UWCCC Experimental Pathology Laboratory for processing harvested tissue for embedding and sectioning. We thank Dr. Norman Drinkwater (UW-Madison) for helpful advice in performing statistical analyses.

FUNDING SOURCES:

This work was supported by funding from the National Cancer Institute to PFL (R35CA210807, P01CA022443) and MES (R50CA211246).

REFERENCES:

Arbeit JM, Howley PM, Hanahan D, 1996 Chronic estrogen-induced cervical and vaginal squamous carcinogenesis in human papillomavirus type 16 transgenic mice. Proc Natl Acad Sci U S A 93, 2930–2935. [PubMed: 8610145]

Bernard HU, Burk RD, Chen Z, van Doorslaer K, zur Hausen H, de Villiers EM, 2010 Classification of papillomaviruses (PVs) based on 189 PV types and proposal of taxonomic amendments. Virology 401, 70–79. [PubMed: 20206957]

Bouvard V, Matlashewski G, Gu ZM, Storey A, Banks L, 1994 The human papillomavirus type 16 E5 gene cooperates with the E7 gene to stimulate proliferation of primary cells and increases viral gene expression. Virology 203, 73–80. [PubMed: 8030286]

Brake T, Lambert PF, 2005 Estrogen contributes to the onset, persistence, and malignant progression of cervical cancer in a human papillomavirus-transgenic mouse model. Proceedings of the National Academy of Sciences of the United States of America 102, 2490–2495. [PubMed: 15699322]

Bubb V, McCance DJ, Schlegel R, 1988 DNA sequence of the HPV-16 E5 ORF and the structural conservation of its encoded protein. Virology 163, 243–246. [PubMed: 2831662]

Chung SH, Wiedmeyer K, Shai A, Korach KS, Lambert PF, 2008 Requirement for estrogen receptor alpha in a mouse model for human papillomavirus-associated cervical cancer. Cancer Res 68, 9928–9934. [PubMed: 19047174]

Conrad M, Bubb VJ, Schlegel R, 1993 The human papillomavirus type 6 and 16 E5 proteins are membrane-associated proteins which associate with the 16-kilodalton pore-forming protein. J Virol 67, 6170–6178. [PubMed: 7690419]

Crusius K, Auvinen E, Steuer B, Gaissert H, Alonso A, 1998 The human papillomavirus type 16 E5-protein modulates ligand-dependent activation of the EGF receptor family in the human epithelial cell line HaCaT. Experimental cell research 241, 76–83. [PubMed: 9633515]

de Villiers EM, Fauquet C, Broker TR, Bernard HU, zur Hausen H, 2004 Classification of papillomaviruses. Virology 324, 17–27. [PubMed: 15183049]

Disbrow GL, Sunitha I, Baker CC, Hanover J, Schlegel R, 2003 Codon optimization of the HPV-16 E5 gene enhances protein expression. Virology 311, 105–114. [PubMed: 12832208]

Elson DA, Riley RR, Lacey A, Thordarson G, Talamantes FJ, Arbeit JM, 2000 Sensitivity of the cervical transformation zone to estrogen-induced squamous carcinogenesis. Cancer Res 60, 1267–1275. [PubMed: 10728686]

Fehrmann F, Klumpp DJ, Laimins LA, 2003 Human papillomavirus type 31 E5 protein supports cell cycle progression and activates late viral functions upon epithelial differentiation. Journal of virology 77, 2819–2831. [PubMed: 12584305]

Genther SM, Sterling S, Duensing S, Munger K, Sattler C, Lambert PF, 2003 Quantitative role of the human papillomavirus type 16 E5 gene during the productive stage of the viral life cycle. Journal of virology 77, 2832–2842. [PubMed: 12584306]

Genther Williams SM, Disbrow GL, Schlegel R, Lee D, Threadgill DW, Lambert PF, 2005 Requirement of epidermal growth factor receptor for hyperplasia induced by E5, a high-risk human papillomavirus oncogene. Cancer research 65, 6534–6542. [PubMed: 16061632]

Gu Z, Matlashewski G, 1995 Effect of human papillomavirus type 16 oncogenes on MAP kinase activity. J Virol 69, 8051–8056. [PubMed: 7494320]

Halbert CL, Galloway DA, 1988 Identification of the E5 open reading frame of human papillomavirus type 16. J Virol 62, 1071–1075. [PubMed: 2828656]

Handisurya A, Day PM, Thompson CD, Buck CB, Pang YY, Lowy DR, Schiller JT, 2013 Characterization of Mus musculus papillomavirus 1 infection in situ reveals an unusual pattern of late gene expression and capsid protein localization. Journal of virology 87, 13214–13225. [PubMed: 24067981]

Hawley-Nelson P, Vousden KH, Hubbert NL, Lowy DR, Schiller JT, 1989 HPV16 E6 and E7 proteins cooperate to immortalize human foreskin keratinocytes. The EMBO journal 8, 3905–3910. [PubMed: 2555178]

Ingle A, Ghim S, Joh J, Chepkoech I, Bennett Jenson A, Sundberg JP, 2011 Novel laboratory mouse papillomavirus (MusPV) infection. Veterinary pathology 48, 500–505. [PubMed: 20685915]

Jiang RT, Wang JW, Peng S, Huang TC, Wang C, Cannella F, Chang YN, Viscidi RP, Best SRA, Hung CF, Roden RBS, 2017 Spontaneous and Vaccine-Induced Clearance of Mus Musculus Papillomavirus 1 Infection. Journal of virology 91.

Lambert PF, Pan H, Pitot HC, Liem A, Jackson M, Griep AE, 1993 Epidermal cancer associated with expression of human papillomavirus type 16 E6 and E7 oncogenes in the skin of transgenic mice. Proc Natl Acad Sci U S A 90, 5583–5587. [PubMed: 8390671]

Lazarczyk M, Pons C, Mendoza JA, Cassonnet P, Jacob Y, Favre M, 2008 Regulation of cellular zinc balance as a potential mechanism of EVER-mediated protection against pathogenesis by cutaneous oncogenic human papillomaviruses. The Journal of experimental medicine 205, 35–42. [PubMed: 18158319]

Leechanachai P, Banks L, Moreau F, Matlashewski G, 1992 The E5 gene from human papillomavirus type 16 is an oncogene which enhances growth factor-mediated signal transduction to the nucleus. Oncogene 7, 19–25. [PubMed: 1311062]

Leptak C, Ramon y Cajal S, Kulke R, Horwitz BH, Riese DJ 2nd, Dotto GP, DiMaio D, 1991 Tumorigenic transformation of murine keratinocytes by the E5 genes of bovine papillomavirus type 1 and human papillomavirus type 16. J Virol 65, 7078–7083. [PubMed: 1658398]

Maufort JP, Shai A, Pitot HC, Lambert PF, 2010 A role for HPV16 E5 in cervical carcinogenesis. Cancer Res 70, 2924–2931. [PubMed: 20332225]

Maufort JP, Williams SM, Pitot HC, Lambert PF, 2007 Human papillomavirus 16 E5 oncogene contributes to two stages of skin carcinogenesis. Cancer Res 67, 6106–6112. [PubMed: 17616666]

Munger K, Phelps WC, Bubb V, Howley PM, Schlegel R, 1989 The E6 and E7 genes of the human papillomavirus type 16 together are necessary and sufficient for transformation of primary human keratinocytes. J Virol 63, 4417–4421.s [PubMed: 2476573]

Pim D, Collins M, Banks L, 1992 Human papillomavirus type 16 E5 gene stimulates the transforming activity of the epidermal growth factor receptor. Oncogene 7, 27–32. [PubMed: 1311063]

Pyeon D, Pearce SM, Lank SM, Ahlquist P, Lambert PF, 2009 Establishment of human papillomavirus infection requires cell cycle progression. PLoS Pathog 5, e1000318. [PubMed: 19247434]

Riley RR, Duensing S, Brake T, Munger K, Lambert PF, Arbeit JM, 2003 Dissection of human papillomavirus E6 and E7 function in transgenic mouse models of cervical carcinogenesis. Cancer Res 63, 4862–4871. [PubMed: 12941807]

Scott ML, Woodby BL, Ulicny J, Raikhy G, Orr AW, Songock WK, Bodily JM, 2019 Human papillomavirus type 16 E5 inhibits interferon signaling and supports episomal viral maintenance. Journal of virology.

Spurgeon ME, Uberoi A, McGregor SM, Wei T, Ward-Shaw E, Lambert PF, 2019 A Novel In Vivo Infection Model To Study Papillomavirus-Mediated Disease of the Female Reproductive Tract. mBio 10.

Straight SW, Hinkle PM, Jewers RJ, McCance DJ, 1993 The E5 oncoprotein of human papillomavirus type 16 transforms fibroblasts and effects the downregulation of the epidermal growth factor receptor in keratinocytes. J Virol 67, 4521–4532. [PubMed: 8392596]

Sundberg JP, Stearns TM, Joh J, Proctor M, Ingle A, Silva KA, Dadras SS, Jenson AB, Ghim SJ, 2014 Immune status, strain background, and anatomic site of inoculation affect mouse papillomavirus (MmuPV1) induction of exophytic papillomas or endophytic trichoblastomas. PloS one 9, e113582. [PubMed: 25474466]

Tomakidi P, Cheng H, Kohl A, Komposch G, Alonso A, 2000 Modulation of the epidermal growth factor receptor by the human papillomavirus type 16 E5 protein in raft cultures of human keratinocytes. European journal of cell biology 79, 407–412. [PubMed: 10928456]

Uberoi A, Yoshida S, Frazer IH, Pitot HC, Lambert PF, 2016 Role of Ultraviolet Radiation in Papillomavirus-Induced Disease. PLoS pathogens 12, e1005664. [PubMed: 27244228]

Valle GF, Banks L, 1995 The human papillomavirus (HPV)-6 and HPV-16 E5 proteins cooperate with HPV-16 E7 in the transformation of primary rodent cells. J Gen Virol 76 (Pt 5), 1239–1245. [PubMed: 7730808]

Wang JW, Jiang R, Peng S, Chang YN, Hung CF, Roden RB, 2015 Immunologic Control of Mus musculus Papillomavirus Type 1. PLoS pathogens 11, e1005243. [PubMed: 26495972]

Zhang B, Li P, Wang E, Brahmi Z, Dunn KW, Blum JS, Roman A, 2003 The E5 protein of human papillomavirus type 16 perturbs MHC class II antigen maturation in human foreskin keratinocytes treated with interferon-gamma. Virology 310, 100–108. [PubMed: 12788634]

Zhang B, Srirangam A, Potter DA, Roman A, 2005 HPV16 E5 protein disrupts the c-Cbl-EGFR interaction and EGFR ubiquitination in human foreskin keratinocytes. Oncogene 24, 2585–2588. [PubMed: 15735736]

zur Hausen H, 2002 Papillomaviruses and cancer: from basic studies to clinical application. Nature reviews. Cancer 2, 342–350. [PubMed: 12044010]

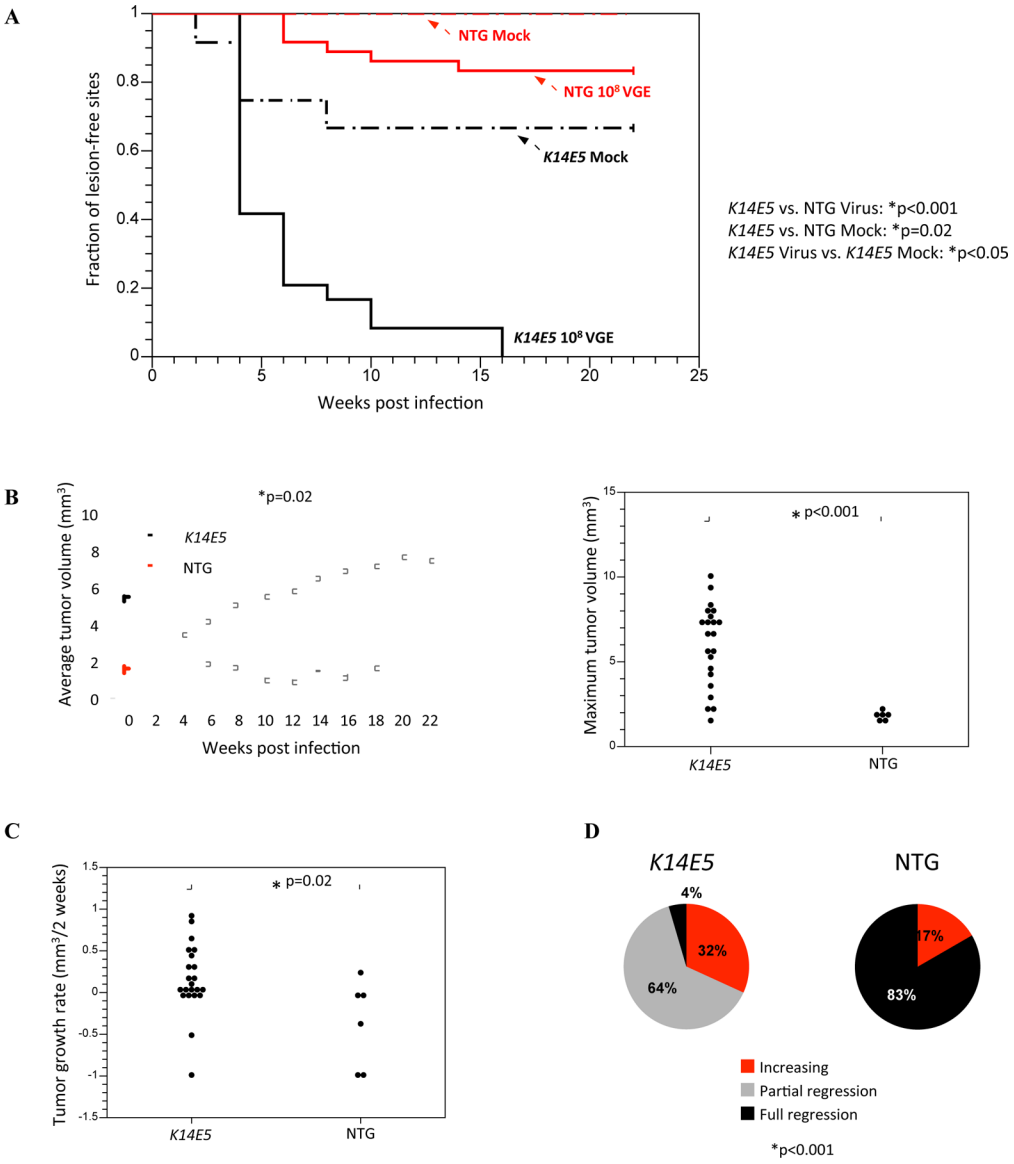

Figure 1. Tumor onset, growth, and regression characteristics in mock-infected and MmuPV1-infected *K14E5* and non-transgenic mice treated with UVB.

(A) Onset of overt lesions on the ears and tails were monitored every other week over a period of 22 weeks post-infection. Mock-infected sites were wounded to induce scarification and topically treated with PBS, then 24 hours later irradiated with UVB. A total of 12 sites were mock-infected on both non-transgenic and *K14E5* mice. MmuPV1-infected sites were wounded to induce scarification and topically treated with MmuPV1 virions (10^8 viral genome equivalents; VGE), then 24 hours later irradiated with UVB. A total of 36 sites were MmuPV1-infected on non-transgenic mice and 24 sites were MmuPV1-infected on *K14E5* mice. MmuPV1-infected lesions in *K14E5* mice displayed a significantly earlier onset than MmuPV1-infected lesions in non-transgenic mice ($p<0.001$) as well as mock-infected lesions in *K14E5* mice ($p<0.02$). While lesions arose in mock-infected *K14E5* mice, no lesions arose in mock-infected non-transgenic mice. All statistical comparisons were performed using a Logrank test. ***(B)*** Overt lesions on the ears and tails were measured every

other week over a period of 22 weeks post-infection (left graph). Lesions that arose in MmuPV1-infected *K14E5* mice were significantly larger in volume over the course of the study than those that arose in MmuPV1-infected non-transgenic mice (*p=0.02, Sen-Adichie test). The maximum tumor volumes of MmuPV1-infected *K14E5* mice were significantly larger than those in MmuPV1-infected non-transgenic mice (*p<0.001, Kruskal-Wallis test) (right graph). ***(C)*** Tumor growth rate was calculated by determining the rate of growth between the time of tumor onset and the next measurement two weeks later. Lesions that arose in MmuPV1-infected *K14E5* mice grew significantly faster than those that arose in MmuPV1-infected non-transgenic mice (*p=0.02, Kruskal-Wallis test). ***(D)*** The extent of tumor regression at the study endpoint was noted for each individual tumor. A tumor is “increasing” if its largest volume measurement was its last one (at 22 weeks). A tumor that has “partially regressed” had reached its greatest tumor volume at some point during the middle of the study but a lesion still remained at the study endpoint. A tumor that has “fully regressed” had appeared during the study but was no longer overtly present at the study endpoint. Pie charts indicate the percentage of tumors in each category. MmuPV1-infected lesions that appeared on non-transgenic mice displayed significantly greater tumor regression than those that appeared on *K14E5* mice. (*p<0.001, Wilcoxon rank sum).

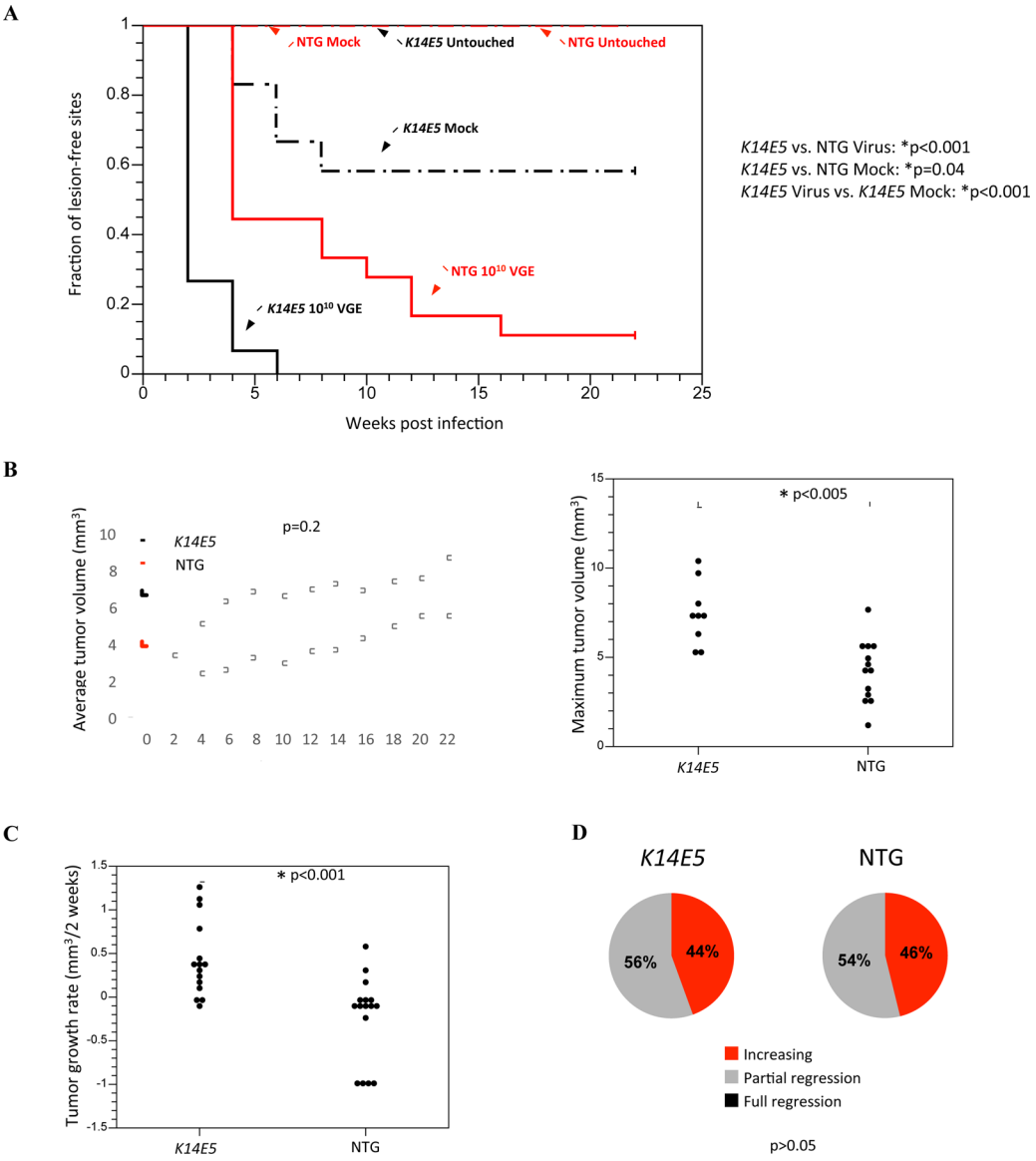

Figure 2. Tumor onset, growth, and regression characteristics in mock-infected and MmuPV1-infected *K14E5* and non-transgenic mice not treated with UVB.

Onset of papillomas that arose on the ears and tails were monitored every other week over a period of 22 weeks post-infection. Untouched sites indicated sites that were not wounded or treated with any solution. Mock-infected sites were wounded to induce scarification and topically treated with PBS. A total of 6 sites were mock-infected on non-transgenic mice and 12 sites were mock-infected on *K14E5* mice. MmuPV1-infected sites were wounded to induce scarification and topically treated with a high dose of MmuPV1 virions (10^{10} viral genome equivalents; VGE). A total of 18 sites were MmuPV1-infected on non-transgenic mice and 15 sites were MmuPV1-infected on *K14E5* mice. MmuPV1-infected lesions in *K14E5* mice displayed a significantly earlier onset than MmuPV1-infected lesions in non-transgenic mice (*p<0.001) as well as mock-infected lesions in *K14E5* mice (*p=0.04). While lesions arose in mock-infected *K14E5* mice, no lesions arose in mock-infected non-transgenic mice. All statistical comparisons were performed using a Logrank test. ***(B)*** Overt

lesions on the ears and tails were measured every other week over a period of 22 weeks post-infection (left graph). There was no significant difference in average tumor volumes of lesions that arose in MmuPV1-infected *K14E5* mice compared to non-transgenic mice ($p=0.2$, Sen-Adichie test). The maximum tumor volumes of MmuPV1-infected *K14E5* mice were significantly larger than those in MmuPV1-infected non-transgenic mice (*$p<0.005$, Kruskal-Wallis test) (right graph). ***(C)*** Lesions that arose in MmuPV1-infected *K14E5* mice grew significantly faster than those that arose in MmuPV1-infected non-transgenic mice (*$p<0.001$, Kruskal-Wallis test). ***(D)*** MmuPV1-infected lesions that appeared on non-transgenic mice did not display significantly greater tumor regression than those that appeared on *K14E5* mice. Pie charts indicate the percentage of tumors in each category. ($p>0.05$, Wilcoxon rank sum).

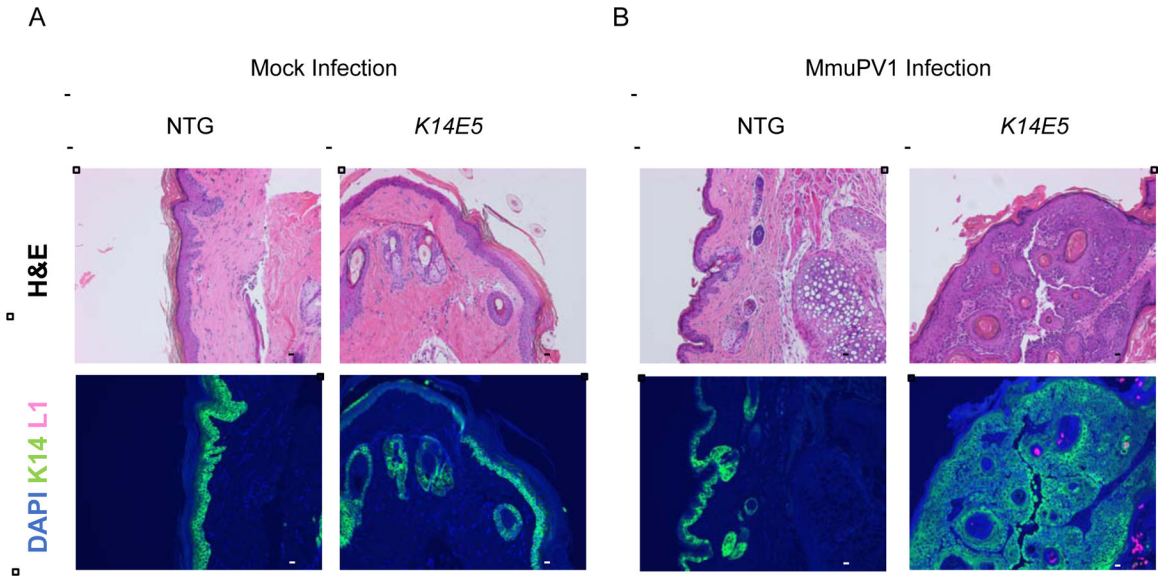

Figure 3. Histopathological analysis of MmuPV1-infected (10^8 VGE) and mock-infected *K14E5* and non-transgenic mice treated with UVB.

To assess whether a productive MmuPV1 infection was present in UVB-irradiated, mock-infected ***(A)*** and MmuPV1-infected ***(B)*** tissue sections from non-transgenic and *K14E5* mice were stained for MmuPV1 L1 capsid protein and cytokeratin 14 protein. Green (AF488): KRT14, Red/Pink (AF647): MmuPV1 L1, Blue: DAPI nuclear stain. Images are at 10X magnification. An adjacent tissue section to that used for immunofluorescent analysis was stained with hematoxylin & eosin (H&E) to show histopathological characteristics of each region. All scale bars = 100 μM.

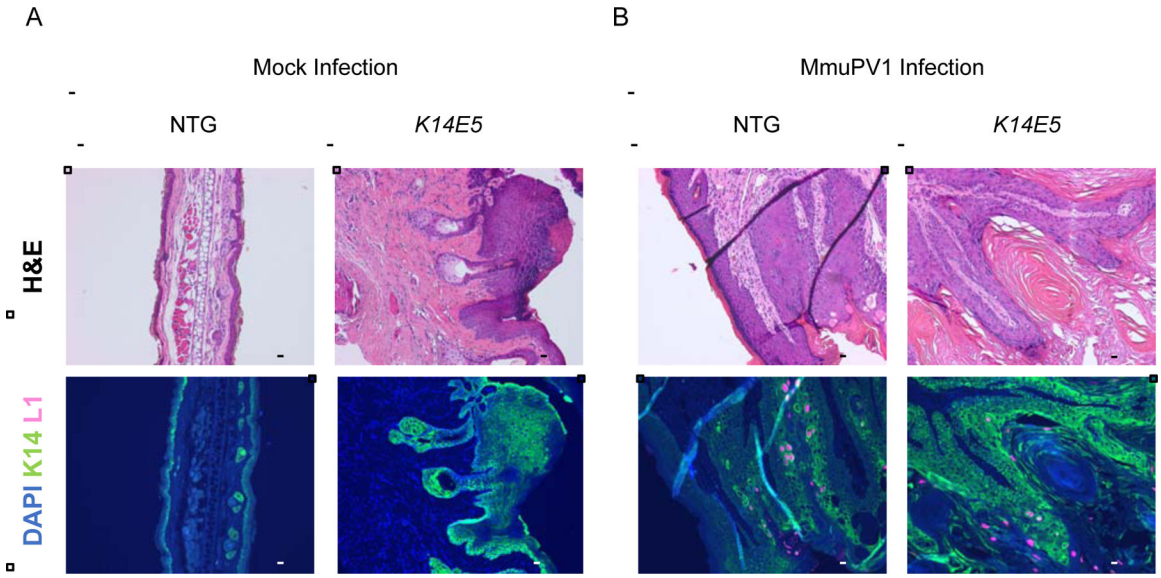

Figure 4. Histopathological analysis of MmuPV1-infected (10^{10} VGE) and mock-infected *K14E5* and non-transgenic mice not treated with UVB.

To assess whether a productive MmuPV1 infection was present in non UVB-irradiated, mock-infected ***(A)*** and MmuPV1-infected ***(B)*** tissue sections from non-transgenic and *K14E5* mice were stained for were stained for MmuPV1 L1 capsid protein and cytokeratin 14 protein. Green (AF488): KRT14, Red/Pink (AF647): MmuPV1 L1, Blue: DAPI nuclear stain. Images are at 10X magnification. An adjacent tissue section to that used for immunofluorescent analysis was stained with hematoxylin & eosin (H&E) to show histopathological characteristics of each region. All scale bars = 100 μM.

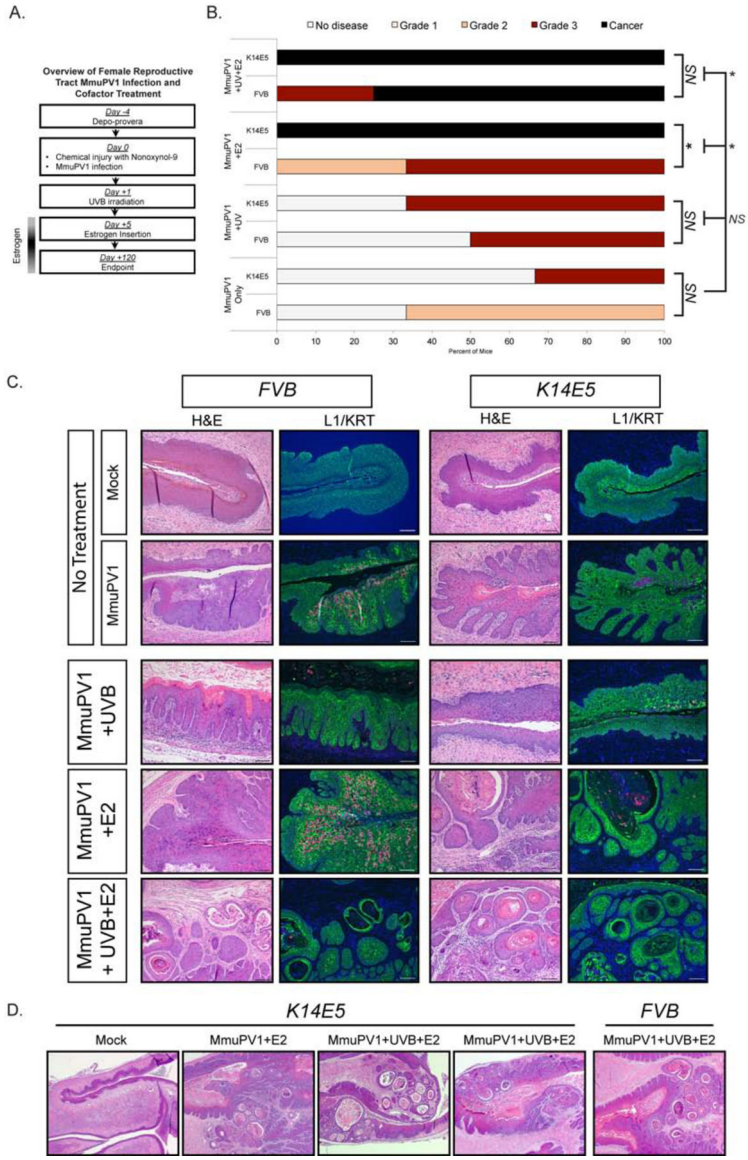

Figure 5. HPV16 E5 gene expression exacerbates disease in estrogen-treated MmuPV1-infected female reproductive tracts of *K14E5* transgenic mice.

(*A*) Overview of female reproductive tract MmuPV1 infection and cofactor treatment. **(*B*)** Cervicovaginal disease severity in *FVB* and *K14E5* mice infected with MmuPV1 only, MmuPV1+UVB, MmuPV1+E2, and MmuPV1+UVB+E2. Two-sided Wilcoxon Rank Sum test was used to compare overall disease severity among groups. An asterisk indicates p-value=0.05. **(*C*)** Representative H&E stained images and immunofluorescence for L1 and Keratin 14 (KRT) for MmuPV1-infected *FVB* (left panels) and *K14E5* (right panels) mice and mock-infected controls. Green (AF488): KRT, Red/Pink (AF647): MmuPV1 L1, Blue: DAPI nuclear stain. Images are at 10X magnification. All scale bars=100 μM. **(*D*)** Comparison of worst disease in MmuPV1-infected *FVB* and *K14E5* mice. Low-magnification (2.5X) images of representative H&E-stained tissues showing a mock-infected *K14E5* mouse and high-grade dysplasias and SCCs arising in MmuPV1+E2 and MmuPV1+UVB+E2 *K14E5* mice. High-grade dysplasia and SCC is shown for

MmuPV1+UVB+E2 *FVB* mouse for comparison, as this was the only condition that gave rise to this level of disease at 4 months post-infection.

Table 1.

Histopathological analysis of tissue samples

UVB-irradiated (10^8 VGE)

Treatment group	*Genotype*	# of sites, n	Disease grade of overt lesion, n (%)						
					Grade of dysplasia			Grade of SCC	
			No disease	Keratosis	Low	Moderate	High	Minimally invasive	Invasive
Mock-infected sites	***NTG***	3	3 (100)						
	K14E5	3	2 (67)	1(33)					
MmuPV1-infected sites	***NTG***	5	5 (100)						
	K14E5	8	1 (12.5)		1 (12.5)		1 (12.5)	1 (12.5)	4 (50)

Non UVB-irradiated (10^{10} VGE)

Treatment group	*Genotype*	# of sites, n	Disease grade of overt lesion, n (%)						
					Grade of dysplasia			Grade of SCC	
			No disease	Keratosis	Low	Moderate	High	Minimally invasive	Invasive
Mock-infected sites	***NTG***	5	5 (100)						
	K14E5	8	5 (62)		3 (38)				
MmuPV1-infected sites	***NTG***	6	1 (17)				3 (50)		2 (33)
	K14E5	6				2 (33)	1 (17)		3 (50)

NOTE: MmuPV1-infected *K14E5* mice displayed increased disease severity versus MmuPV1-infected non-transgenic mice in UVB-irradiated ($p<0.01$) but not in non UVB-irradiated treatment groups ($p=0.4$). All statistical analysis was performed using a two-sided Wilcoxon rank sum test.